Al-Mustansiriyah Journal of Science
ISSN: 1814-635X (print) 2521-3520 (electronic)

ORIGINAL ARTICLE OPEN ACCESS

Antioxidant and Anticancer Activities of Silver Nanoparticles Synthesized Using Cinnamon Extracts

Khalidah Khalaf Jabbar [a], and Mohamed Bouaziz [b]

[a] Al-Ghazali Intermediate School for Boys, Ministry of Education, Iraq
[b] Laboratory of Electrochemistry and Environment, National School of Engineers of Sfax, University of Sfax, Tunisia

CORRESPONDENCE
Khalidah Khalaf Jabbar
Khalidah.Jabbar@gmail.com

ARTICLE INFO
Received: April 06, 2025
Revised: June 02, 2025
Accepted: June 11, 2025
Published: June 30, 2025

ABSTRACT: ***Background:*** *There is great interest in developing plant-based nanoparticles due to their unique chemical and physical properties, which make them an excellent alternative to chemical drugs that fight bacteria and protect cells from damage.* ***Objective:*** *Green synthesis of silver nanoparticles using cinnamon, characterization and evaluation of them as antioxidants, and investigation of their effect on the HepG-2 cell line.* ***Methods:*** *The study involved the green synthesis of Ag NPs/cinnamon, its characterization using XRD, TEM, and GC-MS techniques, and the evaluation of its activity as DPPH antioxidants as well as activity against the HepG-2 cell line.* ***Results:*** *During analysis, it was found that the diameter of the nanoparticles ranged from approximately 19 to 100 nm. The results indicated that the crystal sizes ranged from 12.68 to 29.76 nm, with an average crystal size of 22.335 nm. Cinnamon contains 25 chemical compounds with high antioxidant activity, such as 3-phenyl-(cinnamaldehyde), coumarin, cis-calamine, trans-calamine, oleic acid, (Z)-9-octadecenoic acid, and octadecenoic-9-enoic acid. The nanoparticles inhibited 62% of free radicals, confirming that Ag NPs/cinnamon has good free radical scavenging activity at low concentrations and can function as antioxidants. The results showed that Ag NPs/cinnamon induced greater damage to HepG-2 hepatocytes than to HFF hepatocytes. At a concentration of 1 mg/ml, silver nanoparticles inhibited cytotoxicity and increased cell viability. Compared with the control group (HFF), the IC_{50} value was 48.41 mg/ml, and the toxicity was 105.1 mg/ml, respectively.* ***Conclusions:*** *Silver nanoparticles combined with cinnamon exhibited significant antioxidant properties, indicating their potential as promising free radical scavengers. Additionally, the synthesized Ag NPs/Cinnamon exhibited notable activity against the HepG-2 cell line.*

KEYWORDS: *Ag NPs; Cinnamon; TEM; DPPH; HepG-2 cell line*

INTRODUCTION

Nanoparticles exhibit unique chemical and physical properties due to their small size and biological, industrial, and agricultural functions [1]. They also feature an active surface, which distinguishes them due to their strong interactions with materials. Natural plants use reducing agents to convert silver ions into nanoparticles of various sizes and shapes [2]. The effectiveness of silver nanoparticles stems from their ability to reach their molecular target and catalyze specific biochemical reactions. Their unique physical and chemical properties, coupled with their small size (less than 100 nm) and high surface-to-volume ratio, make them a strong candidate for anticancer applications [3]. Their low toxicity makes them an attractive candidate for alternative anticancer agents. These materials are likely to disrupt the mitochondrial respiratory chain, potentially reducing reactive oxygen species (ROS) and free radical scavenging [4]. Green Nano synthesis is an alternative treatment due to its high efficacy and low cost compared to traditional chemical treatments. Plants and herbs are major sources of essential fatty acids, including omega-3 and omega-6, as well as vitamins and fiber, and are the primary sources of carbohydrates that improve liver and digestive system function [5]. In recent studies and techniques, research has focused on finding effective alternatives

to traditional drugs due to their resistance, as they work against free radicals and toxic cells. As a result, this has contributed to the development of new, effective, and less expensive drugs [6].

The current study used cinnamon, a member of the genus Cinnamomum (Lauriaceae family), known for its ability to slow the action of free radicals and the ageing process through its properties and active chemical compounds, including oleic acid [7], octacosane, calamine, and others [8]. Cinnamon, used in cosmetics, reduces the risk of heart and liver diseases [9]. The study aims to use environmentally friendly plants by preparing silver nanoparticles using cinnamon, characterizing and evaluating them as antioxidants, and studying their effect on the HepG-2 cell line.

MATERIALS AND METHODS

Extraction of Cinnamon

20 g of ground cinnamon was dissolved with 100 ml of 70% ethanol [1 g: 5 ml], and the solution was incubated in a water bath at 37 °C for 20 hours. The extract was filtered using Whatman filter paper and then centrifuged for 10 minutes, kept at 4 °C, and used for further investigations [10].

Biosynthesis of Ag NP/Cinnamon

A volume of 0.5 mL of cinnamon extract was added to 10 mL of a 1 mM aqueous silver nitrate ($AgNO_3$) solution. The resulting particle was then suspension subsequently diluted tenfold with distilled water to mitigate potential inaccuracies arising from the high optical density of the solution. The prepared suspension was stored appropriately and utilized for subsequent experimental investigations [11].

Characterization Techniques

1 X-ray Diffraction (XRD) Analysis of Ag NPs/Cinnamon

The size and crystalline shape of the synthesized silver nanoparticles were determined using an X-ray diffraction (XRD) device (A Phillips X pert PA Holland). The measurements were conducted in Zone 20 over a 2θ range of 4–90°, with a scanning rate of 0.5° per minute and a time constant of 2 seconds The X-ray diffraction profile, which shows the linewidth of the maximum power reflection peak, was used to estimate the average diameter of the formed silver nanoparticle. The Scherrer equation was used to estimate the size of the silver nanoparticles (Ag NPs)/cinnamon [12].

2 TEM

Transmission electron microscope (TEM) (EM208S, Philips, 100kV) was used to determine the structure of the nanoparticles, with images analyzed using Image J software [13].

3 GC-MS of Cinnamon

The chemical composition and molecular mass of the sample were determined. The GC-MS mass spectrum was analyzed against a database of more than 6000 patterns at the National Institute of Standards and Technology (NIST). The nomenclature, mass, and composition of the tested materials were confirmed. We used an Agilent 6890 N (USA) and followed standard procedures to perform GC-MS analysis of silver and cinnamon nanoparticles [14]. The GC-MS instrument was equipped with the HP 5989 mass spectrometer detector. The Agilent 5 MS –HP Column was 30 cm long, 0.025 mm inner diameter, and 0.25 μm particle size. Agilent G1701DA MSD Chem Station software was used for data analysis.

Evaluation of Ag NPs-cinnamon as Antioxidant Agent

DPPH mixed with an organic solvent, the DPPH radical is purple-colored. When it is exposed to a reducing agent, it turns yellow. Any chemical or biological molecule with reducing capabilities can neutralize this radical. A decrease in color intensity at 517 nm indicates an increase in radical neutralization capacity. The percentage of DPPH free radical removal is how the test's results are presented. Kavosh Arya Analytical Company uses Trolox, sold under the trade name Zantox, as a standard in the DPPH kit. One hundred milligrams of DPPH is dissolved in ten milliliters of

ethanol to provide the base solution. Standard concentrations are determined in the range of 0 to 1000 micromoles. Distilled water serves as a blank. Put 10 microliters of the sample (Nano silver-cinnamon), either dissolved or watered down, into each well. Then add the DPPH solution. The absorbance of the sample was then measured at 517 nm in the dark [15].

MTT Assay and IC_{50} Determination of Ag NPs-cinnamon

The viability of cells treated with different concentrations of silver/cinnamon nanoparticles was evaluated using the MTT assay. This colorimetric assay is based on the reduction of the yellow tetrazolium salt [3-(4,5-dimethyl-2-thiazolyl)-2,5-diphenyl-2H-tetrazolium bromide; MTT; Sigma-Aldrich, Darmstadt, Germany] to a blue formazan product by mitochondrial dehydrogenase in metabolically active cells and reflects the metabolic rate of the treated cells. Hepatocytes were cultured in 96-well plates in appropriate culture medium, pre-incubated for 24 h at 37°C containing 5% carbon dioxide. The cells were stimulated for 24 hours with different concentrations of silver/cinnamon nanoparticles in the respective cell culture medium. Then, small amounts of 10 μL of filtered MTT solution (0.22 μM) (0.5 mg/mL) mixed in PBS were added to the wells, and the plates were kept in a dark, humid environment with 5% carbon dioxide for 4 hours at 37 °C. The supernatant was then removed, and 100 μL of dimethyl sulfoxide was added. The plates were mixed horizontally for 15 min, and the optical density was measured at 570 nm (reference wavelength 630 nm). The results were expressed as the percentage of cells in the untreated control group [16], and the percentage of cell viability was calculated according to equation 1.

$$\%Cell\ Viability = \frac{At–Abt}{Ac–Abc} \times 100\%, \tag{1}$$

where, At is the absorbance value of tested Ag NPS/c, Abt is the absorbance value of blank well contained culture medium with the corresponding Ag NP/c concentration, Ac is the absorbance value of control cells, Abc is the absorbance value of blank well contained culture medium.

Then found the IC_{50} which is given by equation 2.

$$IC_{50} = \frac{50 - A}{B - A} \times (D - C) + C, \tag{2}$$

where A is the percentage of inhibition, that is immediately less than 50%, B is the percentage of inhibition, that is immediately greater than or equal to 50%, C is the concentration of inhibit or that gives A% inhibition and D is the concentration of inhibit or that gives B% inhibition.

RESULTS AND DISCUSSION

X-ray Diffraction (XRD) Analysis

When analysis of the synthesized nanoparticles, they were found to consist of four diffraction peaks resulting from X-ray diffraction (XRD) analysis. As shown in Table 1, at an inclination angle of 32.56°, 2 theta, the intensity is 67.74, with a relatively broad peak (FWHM = 0.3936). The corresponding d-spacing is 2.75045 Å, and its relative intensity is 19.46% of the highest peak. The peak at an inclination angle of 38.53° 2 theta is the most intense, with an intensity of 348.07 and a d-spacing of 2.75045 Å. Its relative intensity is 100%, indicating that it is the reference peak. Meanwhile, the peak intensity at 64.73° 2theta is 72.96, its maximum width at its midpoint is 0.3936, its d-spacing is 1.44015 angstroms, and its relative intensity is 20.96%. At 77.71° 2 theta, the peak intensity is 67.35, and its maximum width at its midpoint is 0.84, indicating that it is a wider peak compared to the other peaks. The d spacing here is 1.22779 angstroms, and its relative intensity is 19.35%, as shown in Figure 1. The results, through analysis, indicate the presence of sharp peaks in XRD, The peaks at 38.53°, 64.73°, and 77.96° correspond to the known crystal planes of silver (111), (220), and (311). These peaks are sharp and clear, indicating a regular (crystalline) atomic arrangement [17]. X-ray diffraction, combined with the Scherer equation, is a powerful tool for analyzing the crystal sizes of nanoparticles. By analyzing the various peaks in the X-ray diffraction data (Table 1).

The crystallite size was calculated using Scherer's equation given by equation 3.

$$D = \frac{K\lambda}{\beta \cos\theta}, \tag{3}$$

where D is the crystal size, K is the crystal form factor (usually K=0.9K = 0.9K), λ is the wavelength of the X-rays (usually 0.15406 nm for Cu Kα rays), β is the peak width at half maximum (FWHM) in radians, θ is the half-diffraction angle.

The results indicate that the crystal sizes in this sample range from 12.68 to 29.76 nm, with an average crystal size of 22.335 nm. The results are similar to those achieved by Gaddam *et al.* [18]. For the synthesis of silver nanoparticles (SC-Ag NPs) from Smilax Chenensis root extract, which had an average size of 39.5 nm. These nanoparticles have a high antioxidant activity.

Table 1. Determination of crystallite sizes and interlayer spacing (d spacing) of Ag NPs/Cinnamon from XRD data

2θ (°)	**Intensity (Height)**	**FWHM (°)**	**d-spacing (Å)**	**Relative Intensity (%)**	**Size (nm)**
32.5556	67.74	0.3936	2.75045	19.46	21.95
38.5285	348.07	0.2952	2.75045	100	29.76
64.7306	72.96	0.3936	1.44015	20.96	24.95
77.7149	67.35	0.84	1.22779	19.35	12.68

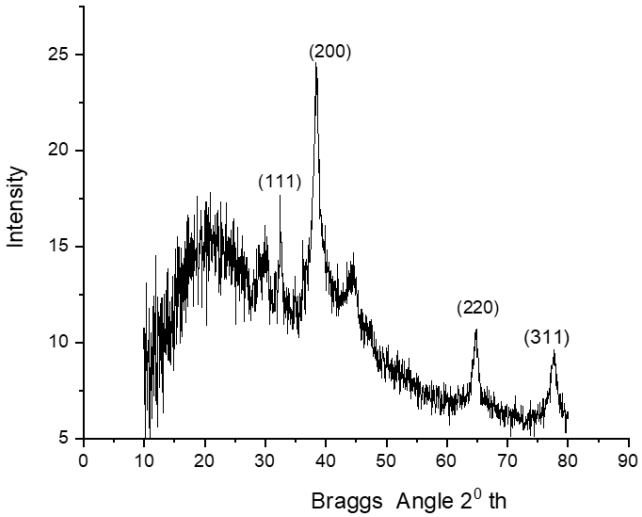

Figure 1. X-ray diffraction (XRD) to determine the crystal structure of Ag NPs/Cinnamon

Gas Chromatography-Mass Spectrometry (GC-MS)

This method separates the volatile components of cinnamon and determines their chemical composition. Figure 2 shows the total ionization chromatography (TIC) of the volatile components over 6 –70 minutes. The results of the volatile component identification are shown in Table 2. Twenty-five chemical compounds were identified, including aldehydes, alcohols, alkanes, and aromatics. The TIC results (Figure 2) showed that the retention times of the active chemical components ranged from 6–56 minutes. Using the NIST11.L mapping library, 25 components were identified by GC-MS. This result indicates that the extraction method significantly impacted the quality and preservation of the volatile components and other chemical compounds in cinnamon. It contained compounds with potent antioxidant and antibacterial properties. The most important of these compounds, listed in Table 2, act as antioxidants: 2-propenal, 3-phenyl- (cinnamaldehyde), coumarin, cis-calaminiene, trans-calaminiene, oleic acid, 9-octadecenoic acid (Z), and octadecene-9-enoic acid. In addition, chemical compounds with antibacterial and anti-inflammatory activity have been found, such as N-hexadecanoic acid (palmitic acid), δ-cadinene, cupine, α-morulin, and others. In a comparative study conducted by Mathew *et al.* [19], cinnamon extract was used for its antibacterial and antioxidant properties. The active compounds were examined after extraction using three different solvents: ethyl acetate, ethanol, and water. The results showed that it contained compounds with antioxidant activity. A study by Owrang *et al.* [20] extracted cinnamon (Cinnamomum zeylanicum) using gas chromatography-mass spectrometry (GC-MS). Analysis revealed six major phytochemicals in CHE, with cinnamaldehyde being the predominant compound. CHE exhibited potent cytotoxicity against the AGS cell line at

concentrations ranging from 100 to 600 μg/ml, significantly reducing the viability of these cancer cells to 20.88% compared to GES-1 cells.

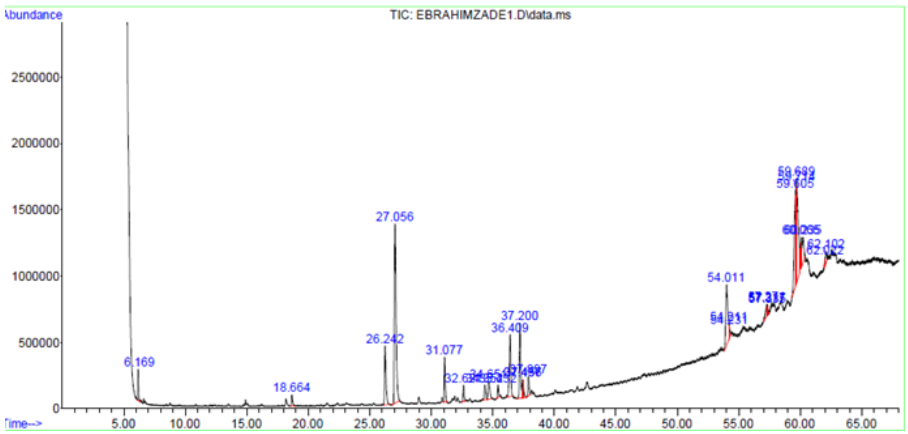

Figure 2. Total ion chromatogram (TIC) of the cinnamon obtained by GC-MS analysis

Table 2. The chemical composition of cinnamon using GC-MS analysis

No	Name of compounds	Formula	Time (min)	Area (%)
1	Benzene, methyl- (CAS)	$C_{18}H_5CH_3$	6.168	1.29
2	Benzaldehyde dimethyl acetal	$C_6H_5CH(OCH_3)_2$	18.661	1.29
3	l-Erythro-2,3-diphenyl)-2-butanol	$C_{16}H_{18}O$	26.24	5.93
4	2-Propenal, 3-phenyl-	C_9H_8O	27.057	22.23
5	Copaene	$C_{15}H_{24}$	31.075	3.39
6	Pyrrolidine, 1-(1-cyclopenten-1-yl)-	$C_9H_{15}N$	32.618	1.27
7	2-Propen-1-ol, 3-phenyl-, acetate, (E)-	$C_{11}H_{12}O_2$	34.35	1.36
8	Coumarin	$C_9H_{60}O_2$	34.653	2.28
9	6.alpha.-Cadina-4,9-diene, (-)-	$C_{15}H_{24}$	35.43	0.92
10	.alpha.-Muurolene	$C_{15}H_{24}$	36.407	6.15
11	delta.-Cadinene	$C_{15}H_{24}$	37.202	6.67
12	cis-Calamenene	$C_{15}H_{22}$	37.436	0.84
13	rans-Calamenene	$C_{15}H_{22}$	37.459	1.06
14	Cubenene	$C_{15}H_{24}$	37.899	1.64
15	n-Hexadecanoic acid	$C_{16}H_{32}O_2$	54.011	8.87
16	Thiosulfuric acid	$C_2H_7NO_3S_2$	54.211	0.25
17	17-Pentatriacontene	$C_{35}H_{70}$	54.233	0.55
18	9-Octadecenoic acid ,(E) -	$C_{18}H_{35}O_5$	57.314	0,27
19	9-Tricosene, (Z)-	$C_{23}H_{48}$	57.337	0.4
20	Oleic Acid	$C_{18}H_{34}O_2$	59.606	9.05
21	9-Octadecenoic acid (Z)-	$C_{18}H_{34}O_2$	59.692	6.77
22	cis-Vaccenic acid	$C_{18}H_{34}O_2$	59.714	11.07
23	Octadec-9-enoic acid	$C_{18}H_{34}O_2$	60.063	1.38
24	Eicosane	$C_{20}H_{42}$	62.023	0.37
25	Octacosane	$C_{28}H_{58}$	62.103	0.85

 DOI: https://doi.org/10.23851/mjs.v36i2.1666

Transmission Electron Microscopy (TEM)

To verify the morphology and size distribution of the biosynthesized Ag NPs/ C, transmission electron microscopy (TEM) analysis was conducted. Representative TEM micrographs are presented in Figure 3 (a, b), illustrating the structural characteristics of the synthesized nanoparticles. The majority of the silver nanoparticles appeared predominantly spherical, with noticeable degrees of agglomeration observed among some particles. Particle size analysis, performed using Image J software, revealed that the nanoparticles ranged in diameter from approximately 1 nm to 100 nm, consistent with findings reported in previous studies [21].

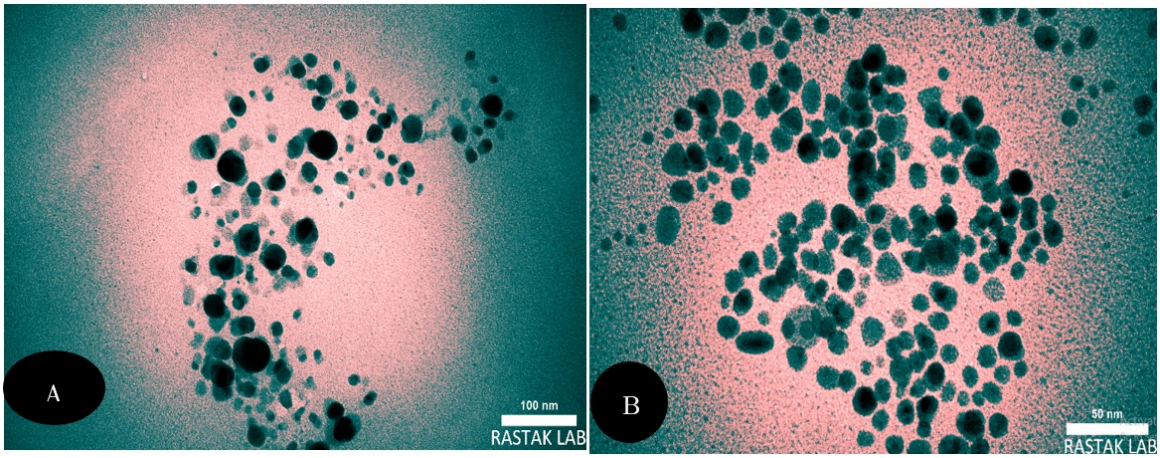

Figure 3. TEM Images of Ag NPs/C. (a) scale bar represents 100 nm, (b) scale bar 50 nm

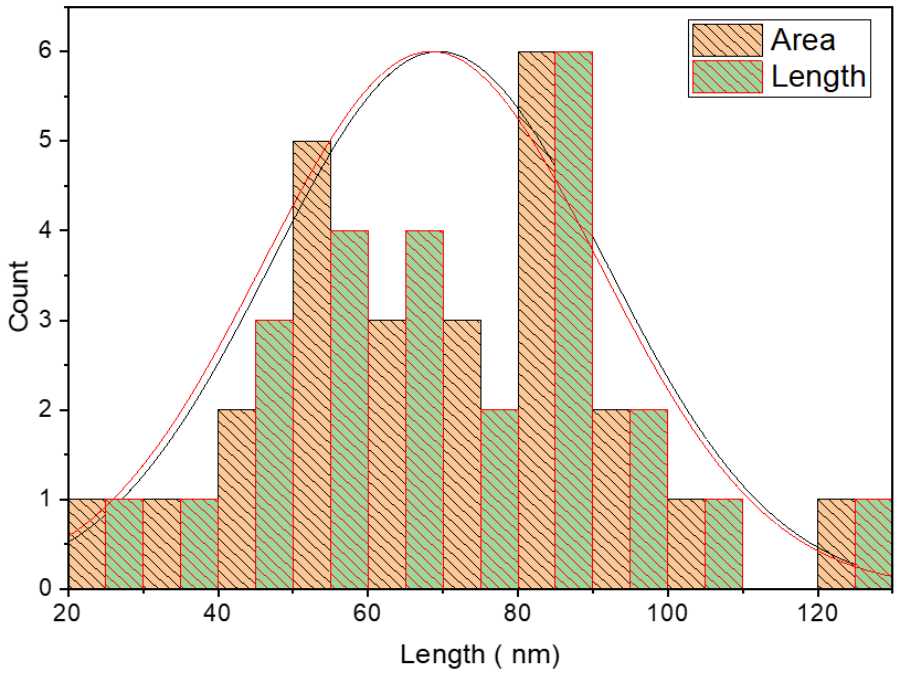

Figure 4. Histogram of nanoparticle size distribution based on length and area measurements

Figure 4 illustrates the size of the nanoparticles, synthesized statistically. A comparison is made between the length and area distributions of the nanoparticles. The analysis aims to understand the distribution pattern and the degree of convergence or divergence between the two variables, area and length. The analytical figure shows a length histogram measured in nanometers (nm), ranging from 20 to 120 nm. The graphical representation also includes two probability density curves, one

representing the length distribution (red) and the other the area distribution (grey), allowing for a direct comparison between the two variables. The data show a distribution pattern close to a normal distribution, with most frequencies concentrated within the 60-90 nm range, with a clear peak at around 70 nm. However, there is a slight deviation in the shape of the distribution, indicating some values above the average. This deviation is likely due to the presence of particles with exceptional lengths or areas. The analysis shows that both length and area follow a distribution close to a normal distribution, with clear centering on the median values and a relatively symmetrical distribution. Slight differences between the two density curves may be attributed to physical factors related to the particle manufacturing process or their structural properties [22].

Anti-oxidation Activity by DPPH Assay

To determine the ability of silver nanoparticles to capture free radicals, an antioxidant activity test was performed. The results are presented, along with the use of ascorbic acid (vitamin C) as a standard. The standard curve illustrates the free radical inhibition effect of the samples used, as shown in Figure 5. The present results indicate that vitamin C and silver nanoparticles can capture free radicals. The study demonstrates that the ability of the nanocomposites to capture free radicals is concentration-dependent, meaning it is dose-dependent. Thus, the highest percentage of captured free radicals was observed at 500 mg/ml for vitamin C (51%), and for silver nanoparticles (21%). On the other hand, the highest percentage of blocked free radicals was observed at 15.6 mg/ml, with the nanoparticles blocking 62%, as shown in Tables 3 and 4.

The results confirm that silver nanoparticles have excellent detoxification activity at the lowest concentrations and can act as antioxidants when vitamin C is used as a reference. The results were similar to those of Wijbauer *et al.* [23] who investigated naturally synthesized silver nanoparticles using aqueous extract of cinnamon tamala leaf (CTAE) that can combat oxidative stress and skin cancer. These particles showed excellent antioxidant activity against free radicals and activity against A375 melanoma cells, with an IC_{50} value of 22 μg/ml. Apoptosis studies demonstrated the superiority of synthetic silver nanoparticles in inducing premature cell death.

Table 3. Antioxidant efficacy of DPPH of ascorbic acid (vitamin C)

Con. of Vit . C	**500 mg/ml**	**250 ml/ml**	**125 mg/ml**	**62.5 mg/ml**	**31.2 mg/ml**	**15.6 mg/ml**
S1	148	155	217	251	271	286
S2	140	148	219	249	268	298
mean	144	151.5	218	250	269.5	292
SD	5.656854	4.949747	1.414214	1.414214	2.12132	8.485281
SEM	4.04061	3.535534	1.010153	1.010153	1.515229	6.060915
% of antioxidant activity	51.10357	48.55688	25.97623	15.11036	8.488964	0.848896

Table 4. Antioxidant efficacy of DPPH of Ag NPs/Cinnamon

Ag NPs/C	**500 mg/ml**	**250 mg/ml**	**125 mg/ml**	**62.5 mg/ml**	**31.2 mg/ml**	**15.6 mg/ml**
S1	232	199	172	183	111	110
S2	231	192	163	173	111	113
mean	231.5	195.5	167.5	178	111	111.5
SD	0.707107	4.949747	6.363961	7.071068	0	2.12132
SEM	0.505076	3.535534	4.545686	5.050763	0	1.515229
% of antioxidant activity	21.39219	33.6163	43.12394	39.55857	62.309	62.13922

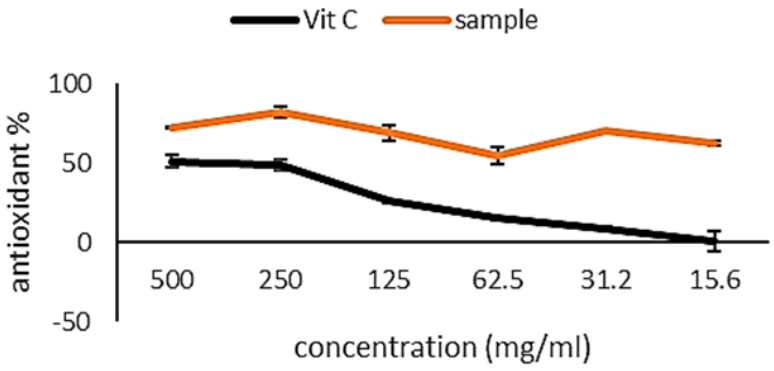

Figure 5. Antioxidant activity of synthetic Ag NPs/C and vitamin C

Measuring Cell Activity by MTT – IC_{50} on HepG-2 Cell Line

Silver nanoparticles/ C can penetrate cancer cells by diffusion or phagocytosis, adhere to the cell membrane, and carry drugs out of the cells. The process lyses harmful cells and causes DNA damage, leading to cell death [24]. Biomolecules synthesized from plant extract play an important role for silver nanoparticles in biological activity. Since cinnamon contains many chemical compounds, the most important of which are acids, we can hope for a positive effect of silver nanoparticles on toxic cells. In a study by others, it has been shown that they can suppress toxic cells by inducing autophagy and apoptosis [25].

Nanoparticles made from cinnamon extract can help combat hepatocellular carcinoma (HepG-2) cell lines and kill toxic cells. We can see the extent to which the synthesized sample cells inhibited the growth of toxic cells using MTT analysis. The results in Tables 5 and 6. It was clear that the silver/C nanoparticles were more harmful to hepatocytes (HepG-2) than to HFF cells, which were used as a control group. At 1 mg/mL, they inhibited the hepatocyte cell line from proliferating and increased cell viability. Compared to the control group (HFF), the IC_{50} value was 48.41 mg/mL, and the toxicity was 105.1 mg/mL, respectively. Thus, the cell viability and anticancer properties can be demonstrated. The graphs and IC_{50} values (concentrations that inhibit the effect at 50%) show that the effect depends on the concentration of added silver nanoparticles; as shown in Figure 6. The results were close to those reached by Muntadhar Sahib *et al.* [26].

Table 5. Measuring cell activity by MTT – IC_{50} on HFF cell line

HFF cell line	**Ctrl**	**1 mg/ml**	**5 mg/ml**	**10 mg/ml**	**25 mg/ml**	**50 mg/ml**	**100 mg/ml**
S1	181	166	156	141	121	111	100
S2	168	178	161	140	112	108	101
S3	160	161	143	158	109	102	89
Mean	169.667	168.333	153.333	146.333	114	107	96.6667
Viability%	100	99.2142	90.3733	86.2475	67.1906	63.0648	56.9745
SD	10.5987	8.7369	9.29157	10.116	6.245	4.58258	6.65833
SEM	6.23455	5.13935	5.46563	5.95059	3.67353	2.69563	3.91666

A decrease in cell viability was observed with increasing concentration, consistent with a dose-response relationship, indicating a concentration-dependent cytotoxic effect.

Linear regression was used to analyze the results using equation 4.

$$y = -0.6564x + 81.766 \tag{4}$$

with an $R^2 = 0.85$, indicating a strong linear correlation between concentration and cell viability within the studied range.

The IC_{50} value was determined to be 48.41 mg/ml, representing the concentration required to inhibit 50% of HepG-2 cell activity.

Table 6. Measuring cell activity by MTT – IC_{50} on HepG-2 cell line

HepG-2 cell line	**Ctrl**	**1 *mg/ml***	**5 mg/ml**	**10 mg/ml**	**25 mg/ml**	**50 mg/ml**	**100 mg/ml**
S1	254	203	204	174	141	98	41
S2	246	185	197	186	134	87	71
S3	232	199	168	157	127	105	63
Mean	244	195.667	189.667	172.333	134	96.6667	58.3333
Viability %	100	80.1913	77.7322	70.6284	54.918	39.6175	23.9071
SD	11.1355	9.45163	19.0875	14.5717	7	9.07377	15.5349
SEM	6.55031	5.55978	11.228	8.57157	4.11765	5.33751	9.13818

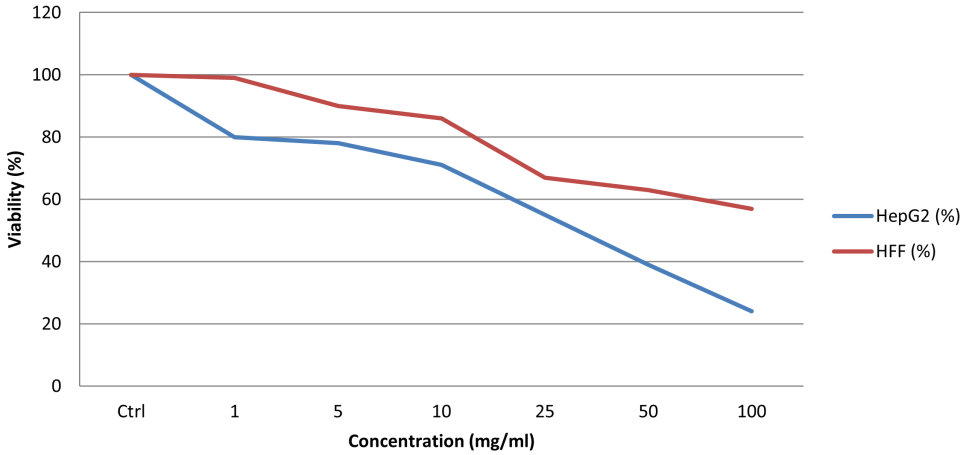

Figure 6. Effect of different concentrations of Ag NPs / C, on the viability of HepG-2 and HFF cells using MTT assay

Figure 6 used the MTT data from Table 4, shows the effects of different concentrations of the compound (1–100 mg/ml) on the viability of hepatocellular carcinoma (HepG-2) cells and normal fibroblast (HFF) cells, highlighting a marked difference in how each cell type reacted. The graph shows the effect of the concentration of silver and cinnamon nanoparticles (mg/ml) on the survival rates of HepG-2 cells (green) and HFF cells (red). The survival rate of HepG-2 cells rapidly decreased from 100% to approximately 23.9071% at 100 mg/ml, while the survival rate of HFF cells decreased slowly, reaching approximately 56.9745% at the same concentration. The viability of HepG-2 cells decreased rapidly with increasing concentration. The curve for HepG-2 intersects the 50% line at approximately 30–35 mg/ml, indicating an IC_{50} value of 48.41 mg/ml. The HFF curve is flatter, indicating greater resistance. The steeper slope of the HepG-2 curve indicates a rapid and detrimental effect of the nanoparticles, a promising sign for selective therapy. The relative resistance of HFF indicates the relative safety of the substance against non-cancer cells. This behavior is attributed to multiple mechanisms, such as the production of reactive oxygen species (ROS). This process allows the nanoparticles to easily penetrate the cancer cell membrane, selectively inducing apoptosis. Finally, the graphs and tables demonstrate that the cinnamon-loaded silver nanoparticles are highly effective and specifically target HepG-2 cancer cells with minimal effect on normal HFF cells. This reinforces their potential as a promising anticancer agent with minimal side effects. Salim *et al.* [27] achieved similar results by using the laser ablation in liquids (PLAL) method to create silver and cinnamon nanoparticles (Ag-CNSs) without any solvents. XRD analysis showed that these nanoparticles have great crystallinity and biological activity. They tested how toxic the nanoparticles were on liver cancer cells (HepG-2) and normal cells (WRL68). The nanoparticles showed anticancer effects with a log IC_{50} of about 59.1%, suggesting they could be effective for treatment.

CONCLUSION

Green synthesis methods for nanomaterials are an emerging field in nanoscience and nanotechnology. Green synthesis methods for nanomaterials are gradually offering solutions to technological and en-

vironmental challenges in the fields of health, industry, and chemical processes. These principles aim to guide the reduction of unsafe products and the optimization of chemical processes. Green silver nanoparticles/ C were synthesized using cinnamon, and the size range was found to be between 19 nm and 100 nm. The cinnamon plant was used to synthesize silver nanoparticles. Cinnamon contains active chemical compounds that make the nanocomposite more biologically active, such as 3-phenyl-(cinnamaldehyde), coumarin, cis-calamine, trans-calamine, oleic acid, (Z)-9-octadecenoic acid, and octadecenoic-9-enoic acid MTT assay results indicate that Ag NPs/ C demonstrated biocompatibility through their resistance to living cell lines. They also demonstrated significant free radical inhibition activity in HepG-2 cells, with an inhibitory concentration (IC_{50}) of approximately 48.41 mg/mL, demonstrating their potential as antioxidants for therapeutic applications. For future studies, the synthesized nanoparticles could be used in a variety of biomedical applications, such as drug delivery systems, accelerating wound healing, and coating medical devices to prevent infection. They can also be used in agriculture as a natural biopesticide to protect crops from fungi and bacteria. They also exhibit antioxidant properties against cancer cells, such as MCF-7 breast cancer cells and cervical cancer cells, by inducing apoptosis and limiting cell proliferation. Silver/cinnamon nanoparticles are a promising tool in modern medicine and warrant further clinical studies.

SUPPLEMENTARY MATERIAL

None.

AUTHOR CONTRIBUTIONS

Khalidah Khalaf Jabbar: Conceptualization, Writing - review, editing, and visualization. Mohamed Bouaziz: Methodology, formal analysis, and validation.

FUNDING

This research received no external funding.

DATA AVAILABILITY STATEMENT

All data in this study are available from the corresponding author with a reasonable request.

ACKNOWLEDGMENTS

The authors would like to thank Universite de Sfax, for its support in completing this work.

CONFLICTS OF INTEREST

The authors declare no conflicts of interest.

REFERENCES

[1] N. Joudeh and D. Linke, "Nanoparticle classification, physicochemical properties, characterization, and applications: a comprehensive review for biologists," *Journal of Nanobiotechnology*, vol. 20, no. 1, p. 262, 2022. doi: 10.1186/s12951-022-01477-8.

[2] M. Asif, R. Yasmin, R. Asif, A. Ambreen, M. Mustafa, and S. Umbreen, "Green synthesis of silver nanoparticles (AgNPs), structural characterization, and their antibacterial potential," *Dose-Response*, vol. 20, no. 2, p. 15593258 221088709, 2022. doi: 10.1177/15593258221088709.

[3] A. V. Samrot, S. P. Ram Singh, R. Deenadhayalan, V. V. Rajesh, S. Padmanaban, and K. Radhakrishnan, "Nanoparticles, a double-edged sword with oxidant as well as antioxidant properties—A review," *Oxygen*, vol. 2, no. 4, pp. 591–604, 2022. doi: 10.3390/oxygen2040039.

[4] M. Oves, M. Ahmar Rauf, M. Aslam, H. A. Qari, H. Sonbol, I. Ahmad, G. Sarwar Zaman, and M. Saeed, "Green synthesis of silver nanoparticles by Conocarpus Lancifolius plant extract and their antimicrobial and anticancer activities," *Saudi Journal of Biological Sciences*, vol. 29, no. 1, pp. 460–471, 2022. doi: 10.1016/j.sjbs.2021.09.007.

[5] A. Dey, A. Mitra, S. Pathak, S. Prasad, A. S. Zhang, H. Zhang, X.-F. Sun, and A. Banerjee, "Recent advancements, limitations, and future perspectives of the use of personalized medicine in treatment of colon cancer," *Technology in Cancer Research & Treatment*, vol. 22, p. 15 330 338 231 178 403, Jan. 2023. doi: 10.1177/15330338231178403.

[6] N. M. Alyami, H. M. Alyami, and R. Almeer, "Using green biosynthesized kaempferol-coated sliver nanoparticles to inhibit cancer cells growth: an in vitro study using hepatocellular carcinoma (HepG2)," *Cancer Nanotechnology*, vol. 13, no. 1, p. 26, 2022. doi: 10.1186/s12645-022-00132-z.

[7] A. Said, M. Abu-Elghait, H. M. Atta, and S. S. Salem, "Antibacterial activity of green synthesized silver nanoparticles using *Lawsonia inermis* against common pathogens from urinary tract infection," *Applied Biochemistry and Biotechnology*, vol. 196, no. 1, pp. 85–98, 2023. doi: 10.1007/s12010-023-04482-1.

[8] Z. Yang, B. Liu, Y. Yang, and D. K. Ferguson, "Phylogeny and taxonomy of *Cinnamomum* (Lauraceae)," *Ecology and Evolution*, vol. 12, no. 10, p. e9378, 2022. doi: 10.1002/ece3.9378.

[9] Z. Sabouri, N. Shakour, M. Sabouri, S. S. Tabrizi Hafez Moghaddas, and M. Darroudi, "Biochemical, structural characterization and assessing the biological effects of cinnamon nanoparticles," *Biotechnology and Bioprocess Engineering*, vol. 29, no. 1, pp. 165–175, 2024. doi: 10.1007/s12257-024-00004-w.

[10] T. S. Sirait, A. Arianto, and A. Dalimunthe, "Phytochemical screening of cinnamon bark (*Cinnamomum burmanii*) (C. Ness & T. Ness) C. Ness ex blume ethanol extract and antioxidant activity test with DPPH (2,2-diphenyl-1-picrylhydrazyl) method," *International Journal of Science, Technology & Management*, vol. 4, no. 1, pp. 254–259, 2023. doi: 10.46729/ijstm.v4i1.739.

[11] A. H. Saliem, O. M. Ibrahim, and S. I. Salih, "Biosynthesis of silver nanoparticles using *Cinnamon zeylanicum* plants bark extract," *Kufa Journal For Veterinary Medical Sciences*, vol. 7, no. 1, pp. 51–63, 2016. doi: 10.36326/kjvs/2016/v7i14294.

[12] G. A. Ismail, N. G. Allam, R. M. Gaafar, M. M. El-zanaty, and P. S. Ateya, "Effect of biologically and chemically synthesized AgNPs on multi-drug resistant (MDR) dermatophyte bacterial isolates," *Egyptian Journal of Botany*, vol. 62, no. 3, pp. 687–707, 2022. doi: 10.21608/ejbo.2022.120076.1905.

[13] T. Mourer, M. Sachse, A. D. Gazi, C. d'Enfert, and S. Bachellier-Bassi, "A protocol for ultrastructural study of *Candida albicans* biofilm using transmission electron microscopy," *STAR Protocols*, vol. 3, no. 3, p. 101 514, 2022. doi: 10.1016/j.xpro.2022.101514.

[14] A. Granja Alvear, N. Pineda-Aguilar, P. Lozano, C. Lárez-Velázquez, G. Suppan, S. Galeas, A. Debut, K. Vizuete, L. De Lima, J. P. Saucedo-Vázquez, F. Alexis, and F. López, "Synergistic antibacterial properties of silver nanoparticles and its reducing agent from cinnamon bark extract," *Bioengineering*, vol. 11, no. 5, p. 517, 2024. doi: 10.3390/bioengineering11050517.

[15] R. B. Hmida, B. Gargouri, and M. Bouaziz, "Chemical changes occur in extra-virgin olive oil during fruits ripeness of zalmati cultivar planted in warm desert climate," *Journal of Oleo Science*, vol. 71, no. 4, pp. 469–479, 2022. doi: 10.5650/jos.ess21342.

[16] M. Wypij, T. Jędrzejewski, J. Trzcińska-Wencel, M. Ostrowski, M. Rai, and P. Golińska, "Green synthesized silver nanoparticles: Antibacterial and anticancer activities, biocompatibility, and analyses of surface-attached proteins," *Frontiers in Microbiology*, vol. 12, Apr. 2021. doi: 10.3389/fmicb.2021.632505.

[17] F. N. Elma, M. Hussain, A. Avcı, E. Pehlivan, S. T. H. Sherazi, and S. Uddin, "Green synthesis of silver nanoparticles mediated by cinnamon extract and its potential insecticidal effect against callosobruchus maculatus (Coleoptera: Chrysomelidae)," *Bitlis Eren Üniversitesi Fen Bilimleri Dergisi*, vol. 14, no. 1, pp. 424–434, 2025. doi: 10.17798/bitlisfen.1596364.

[18] S. A. Gaddam, V. S. Kotakadi, R. Allagadda, V. T., S. G. Velakanti, S. Samanchi, D. Thangellamudi, H. Masarapu, U. Maheswari P, A. R. Ch, and E. A. Zereffa, "Bioinspired multifunctional silver nanoparticles by *Smilax Chenensis* and their enhanced biomedical and catalytic applications," *Scientific Reports*, vol. 14, no. 1, p. 29 909, 2024. doi: 10.1038/s41598-024-77071-9.

[19] O. E. Matthew, F. T. Esther, O. N. Cicilia, A. C. Glory, O. I. Godwin, D. O. Kate, S. K. Garba, O. E. Dorathy, D. O. Kate, and A. C. Glory, "Antibacterial efficacy, *in vitro* antioxidant and GC-MS analyses of cinnamon bark," *International Research Journal*, vol. 10, no. 4, pp. 639–658, 2023. [Online]. Available: https://tijer.org/tijer/papers/TIJER2304228.pdf.

[20] M. Mutlu, Z. Bingol, E. M. Uc, E. Köksal, A. C. Goren, S. H. Alwasel, and İ. Gulcin, "Comprehensive metabolite profiling of Cinnamon (*Cinnamomum zeylanicum*) leaf oil using LC-HR/MS, GC/MS, and GC-FID: determination of antiglaucoma, antioxidant, anticholinergic, and antidiabetic profiles," *Life*, vol. 13, no. 1, p. 136, 2023. doi: 10.3390/life13010136.

[21] S. H. Alwan and M. H. Al-Saeed, "Biosynthesized silver nanoparticles (using *Cinnamomum zeylanicum* bark extract) improve the fertility status of rats with polycystic ovarian syndrome," *Biocatalysis and Agricultural Biotechnology*, vol. 38, p. 102 217, Nov. 2021. doi: 10.1016/j.bcab.2021.102217.

[22] M. A. Al Mashud, M. Moinuzzaman, M. S. Hossain, S. Ahmed, G. Ahsan, A. Reza, R. B. Anwar Ratul, M. H. Uddin, M. A. Momin, and M. A. Hena Mostofa Jamal, "Green synthesis of silver nanoparticles using *Cinnamomum tamala* (Tejpata) leaf and their potential application to control multidrug resistant *Pseudomonas aeruginosa* isolated from hospital drainage water," *Heliyon*, vol. 8, no. 7, p. e09920, 2022. doi: 10.1016/j.heliyon.2022.e09920.

[23] L. S. Vijapur, Y. Srinivas, A. R. Desai, A. S. Gudigennavar, S. L. Shidramshettar, and P. Yaragattimath, "Development of biosynthesized silver nanoparticles from *Cinnamomum tamala* for anti-oxidant, anti-microbial and anti-cancer activity," *Journal of Research in Pharmacy*, vol. 27, no. 2, pp. 769–782, 2023. doi: 10.29228/jrp.359.

[24] H. I. O. Gomes, C. S. M. Martins, and J. A. V. Prior, "Silver nanoparticles as carriers of anticancer drugs for efficient target treatment of cancer cells," *Nanomaterials*, vol. 11, no. 4, p. 964, 2021. doi: 10.3390/nano11040964.

[25] Y. G. El-Baz, A. Moustafa, M. A. Ali, G. E. El-Desoky, S. M. Wabaidur, and M. M. Faisal, "An analysis of the toxicity, antioxidant, and anti-cancer activity of cinnamon silver nanoparticles in comparison with extracts and fractions of cinnamomum cassia at normal and cancer cell levels," *Nanomaterials*, vol. 13, no. 5, p. 945, 2023. doi: 10.3390/nano13050945.

[26] S. Montazersaheb, R. Farahzadi, E. Fathi, M. Alizadeh, S. Abdolalizadeh Amir, A. Khodaei Ardakan, and S. Jafari, "Investigation the apoptotic effect of silver nanoparticles (Ag-NPs) on MDA-MB 231 breast cancer epithelial cells via signaling pathways," *Heliyon*, vol. 10, no. 5, p. e26959, 2024. doi: 10.1016/j.heliyon.2024.e26959.

[27] A. Salim, H. Bakhtiar, D. A. S. Dawood, and S. Ghoshal, "Anticancer and cytotoxicity evaluation of silver-cinnamon nanoshells," *Materials Letters*, vol. 334, p. 133 671, Mar. 2023. doi: 10.1016/j.matlet.2022.133671.